Approaches to Simulating Meta-surfaces for Flat Optical Devices: The Transition to Solutions Based on Neural Networks

Denis RIDEAU[1], Mathys LE GRAND[1], Louis Henri FERNANDEZ MOURON[1,4] Valérie SERRADEIL[1], Loumi TREMAS[1,5], Pascal URARD[1], Damien MAITRE[1], Habib MOHAMAD[2], Lucie DILHAN[1,2], Enrico Giuseppe CARNEMOLLA[3], Matteo FISSORE[3], James DOWNING[3], and Bruce RAE [1,3].

[1] *STMicroelectronics, 850 rue J. Monnet BP16, 38926 Crolles, France ;*
[2] *STMicroelectronics, 12 rue J. Horowitz, 38019 Grenoble, France;*
[3] *STMicroelectronics, 1Tanfield, Inverleigh Row, Edinburgh, UK;*
[4] *Université Paris Dauphine Place du Maréchal de Lattre de Tassigny, 75775 Paris, France ;*
[5] *IOGS Université Paris Saclay,2 Av. Augustin Fresnel, 91120 Palaiseau, France.*

2024 International Conference on Simulation of Semiconductor Processes and Devices (SISPAD) | 979-8-3315-1635-2/24/$31.00 ©2024 IEEE | DOI: 10.1109/SISPAD62626.2024.10733267

***Abstract*— Following a summary of the constraints associated with simulations using pillar-wise-based methods to design meta-surfaces, we will present our latest progress in the domain of simulating large scale meta-surfaces, including convolutional neural network-driven emulations. We highlight the significance of accurately modeling the impact of the interaction between the pillars in a meta-surface, which enables the elimination of meta-surface designs with poor optical performances (e.g. zeroth orders in a beam shaper) during the design verification stages.**

Keywords—Meta-surface, Neural network, Flat optics, Beam shaper, Meta-lenses, Meta-diffuser.

I. INTRODUCTION

A meta-surface consists of nanostructures that are smaller than the wavelength of light and can be utilized to create functional devices with an ultra-thin profile [1][2][3]. Research laboratories using electron beam lithography have demonstrated that a large variety of optical devices, such as a lens, spectral filters, a polarization band pass filter, and a beam shaper (also call hereafter meta-diffuser), can be efficiently replaced by 'flat' meta-surface-based optics. Meta-surfaces are now sufficiently advanced to transition into large-scale production. Semi-conductor companies are preparing for a massive surge in meta-surface technology business in the coming years. To facilitate this shift, it is crucial to employ accurate simulations of optical meta-surfaces and to develop innovative design approaches.

Due to the relatively large dimensions (mm) of these optical systems and the fact that the diffraction patterns are sub-wavelength, well known Electromagnetic simulation techniques based on Finite Difference Time Domain (FDTD) can sometimes be very delicate to implement. For this reason, alternative approaches based on neural networks prove to be very effective and make the simulation of large meta-surfaces possible. After a brief overview of the limitations of the pillar-wise and FDTD based simulations, we will present our recent advancements in the field of Neural-network-based emulation of large meta-surfaces.

The test cases presented in this paper focus on meta-diffusers, but the methods used to design these structures are more general and can apply to different types of meta-surfaces.

II. PERIODIC PILLAR-WISE LIBRARY

Meta-surfaces' adaptability enables versatile designs, and it is possible to obtain a 'nearly' local phase shift (of an incident wave) at the sub-wavelength scale. Indeed, under each diffractive element (typically pillars of high permittivity embedded in a medium of lower permittivity), the incident wave undergoes a phase shift proportional to the width of the latter. A widely used strategy to link the local phase shift below the pillar with its width consists of the use of a look-up table in which the phase below the pillar is tabulated as a function of the width. In general, electromagnetic simulations are performed using a periodic unit-cell composed of a single pillar. The phase and the transmission as a function of the (normalized) pillar widths are shown in Figure 1 a) for a light angle of zero degree. Results are obtained using a commercial 3D-FDTD solver [4]. The phase exhibits a nearly monotonous increase and the transmission remains high apart from narrow drops at well-defined pillar widths. The situation is more complex when the incident light exhibits a non-zero angle as testified by Figure 1 b). This is further exemplified in Figure 2 where we see that depending on the width of the pillar, the structure of the transmission under the meta-surface can be extremely complex.

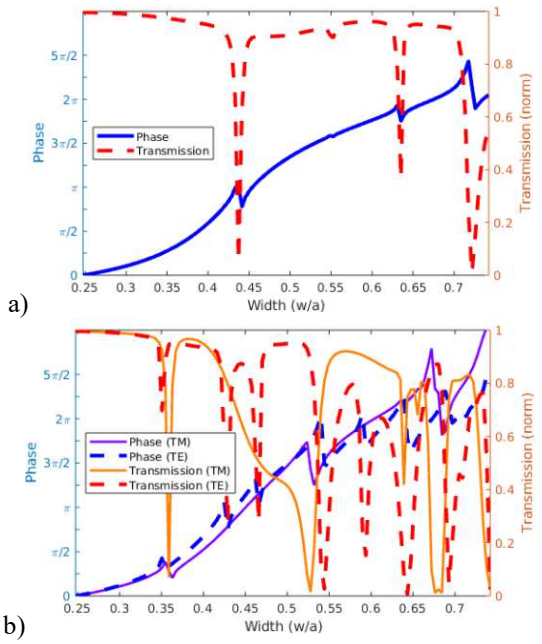

Figure 1: Typical Phase and Transmission for a periodic (of period *a*) meta-surface composed of identical semiconductor pillars of width (*w*) embedded in glass: with an incident light wave length of 940nm, a) at zero degree and b) at 16 degrees (both light polarizations are shown).

As has often been discussed (and sometime referred to as non-local effects [1]), resonances leading to discontinuous phase-width relations and abrupt transmission drops, can occur for well-defined values of the width of the pillars and can be inferred from a coupling between the incident light and transversally-propagating modes. Such coupling occurs when the meta-surface is purely periodic (and composed of rigorously identical pillars). Except in particular 'non-local' systems where resonances are researched, such as in band-pass filters, in meta-lens and beam-shapers, this is generally not the case, and such resonances are likely not to occur (see later).

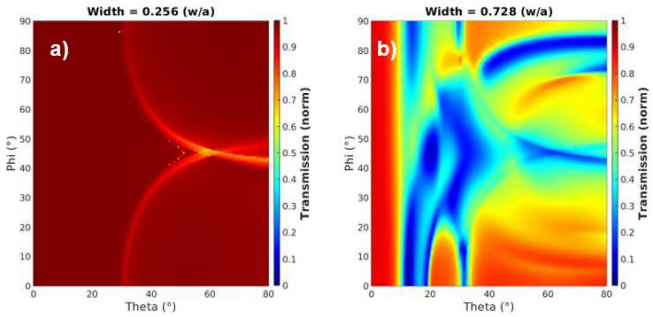

Figure 2: 2-D maps of the Transmission for two different pillars of normalized widths; a) *w/a=0.256 and b) w/a=0.728*. Same periodic meta-surface (of period a) as in Figure 1 for transverse-electric-polarization.

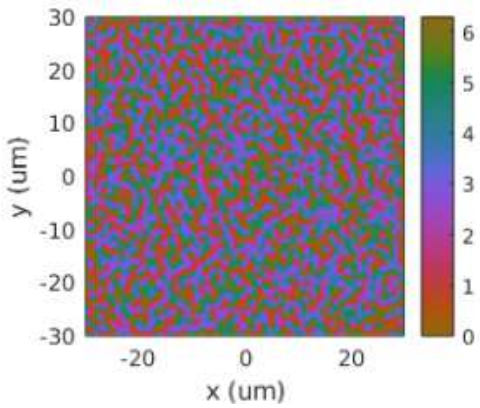

Figure 3: Theoretical phase shift map (128*128 pillars) obtained using a Gerchberg-Saxton-like algorithm [5] in order to target in the far field the arbitrary shape shown in Figure 8 b).

Figure 3 shows the theoretical phase shift obtained using a Gerchberg-Saxton-like algorithm [5] in order to target in the far field the arbitrary poly-shape shown in Figure 8 b). From this phase shift map and using the lock-up table shown in Figure 1 a), a pillar radius map (or width map) can be extracted. We note, incidentally, that due to the discontinuity in the Phase-width relationship, such a 'mapping' function can be ambiguous, and several width values can be extracted for the same phase shift target. Such a situation can lead to a deterioration of the optical performance of the design as shown in Figure 4. The exact same design of a beam shaper is mapped using either the (discontinuous) periodic pillar-wise library or using the (continuous) function related to a random structure shown in Figure 6. As can be seen the far field (1 meter from the meta-diffuser) exhibits a significant zeroth-order (characterized by an intensity maximum at normal incidence) when a purely period mapping function is used. This is not the case with the later continuous function.

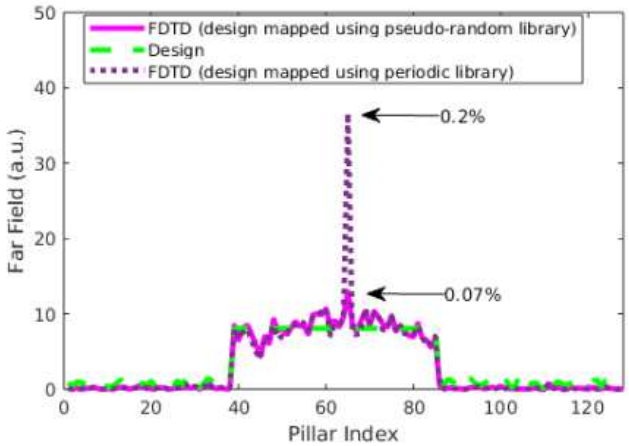

Figure 4: Far field intensity as a function of the pillar index for two meta-diffusers in which the design (the near field phase-shift) is mapped using two different funtions (see texte for detail).

III. A STOCHASTIC APPROACH TO DESIGN BEYOND PERIODIC PILLAR-WISE LIBRARY

To assess the impact of the design on the phase below each pillar, we constructed a large dataset of pseudo-random radius maps with varying correlation lengths. The correlation length, indicating the smoothness of radius transitions between adjacent pillars, is given by $d_{corr}=N*\sigma$, where σ is the gaussian perturbation's standard deviation and N is the number of pillars along the *x*-directions and the y-directions. Figure 5 shows the FDTD near field phase at 50nm from the meta-surface for two pseudo-random radius maps with a) small and b) larger correlation lengths. The meta-surface is illuminated under a normal, monochromatic (940nm), transverse-electric-polarized beam.

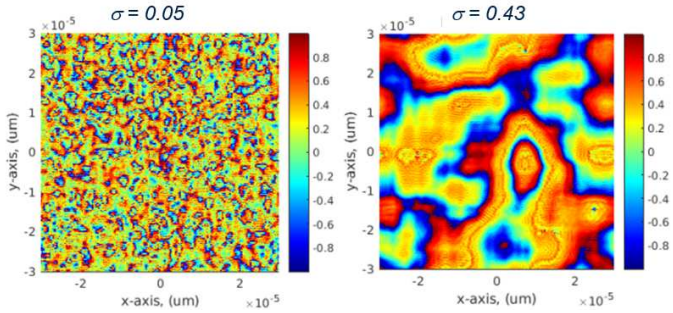

Figure 5: FDTD near field phase at 50nm from the meta-surface for two pseudo-random radius maps with a) small and b) larger correlation lengths.

The 'local' local phase below the pillar is then extracted averaging the FDTD results on the unit-cell around each pillar. We found out that the relationship between the radius of a pillar and the induced local phase change is influenced not only by the parameters of the pillar itself but also by the presence of other pillars nearby. Figure 6 shows the average phase and the transmission as a function of the width below the pillars for various pseudo-random structures. This puts forth how neighboring pillars affect a specific individual pillar local phase and transmission. It is also noted that the resonance amplitudes diminish as the correlation lengths increase. Based on this stochastic analysis of the system a more relevant lock-up table can be built and used instead of the purely periodic one (see Figure 4).

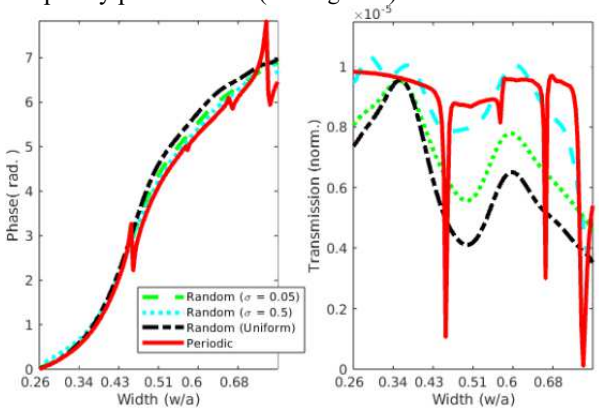

Figure 6: Average phase and transmission as a function of the pillar width for different pseudo-random structures.

IV. EMULATING THE META-SURFACE NEAR FIELD WITH A RESNEXT

From a detailed study of the previously mentioned pseudo-random structures we found out that the influence of neighboring pillars on the local phase below a pillar is complex and can exhibit a long range of interaction (typical up to several tenth of pillars). A possible way to handle such a complexity, in a more accurate way than the previous stochastic model, consists in using convolutional neural networks (CNN) [6]. To perform such a model, a large database (>10k elements) of 20x20 crops of realistic meta-lenses and meta-diffusers is build. The database is composed of 2D images of the electric field 50 nanometers after the meta-surface. In the present meta-surface, the pillars are arranged at half-wavelength intervals. A resolution of one pixel per half wavelength is sufficient to calculate the entire far field according to the Nyquist criterion for propagating waves. The high-resolution near field produced by the FDTD solver is subsequently down-sampled by means of filtering the high-frequency spatial components. The benefits of this down-sampling are twofold. It reduces the neural network's output size by more than 400 times. Additionally, it allows for the use of smaller kernels in the convolutional neural network while maintaining the same physical receptive field size (i.e. the maximum distance from which a kernel can receive information from other pixels).

We found out that ResNeXt architecture [7], originally designed for image-centric input and output, excels in learning the complex patterns of the meta-surface near field more efficiently than Skip-CNN. We believe that its deeper emulated network structure and its parallel convolutional pathways enhance feature extraction, which appears to be crucial for interpreting electromagnetic data. A pictural illustration of the network is shown in Figure 7. The inputs are the width maps and the outputs are the near fields split into two distinct real and imaginary channels. The layers are periodic in order to account for the periodic boundary condition used in the FDTD simulations.

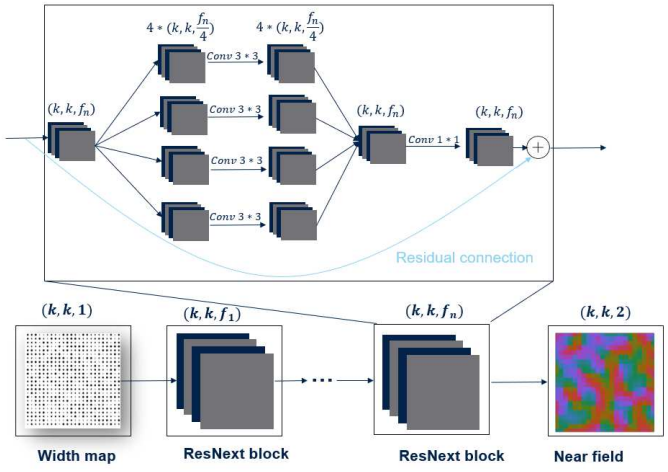

Figure 7: ResNeXt composed of 30 blocks $(k,\ k,\ f_i)$, with size of k=20, and filter number f_i = 128 for all blocks. A block is detailed. The inputs are the width maps, and the outputs are the near fields split into two distinct real and imaginary channels.

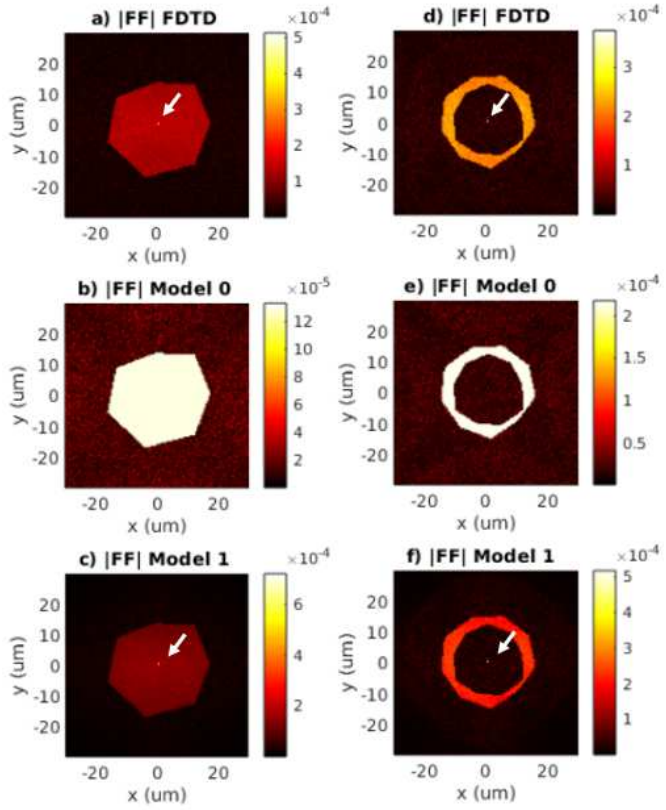

Figure 8: Two beam shapers with arbitrary random poly-shapes (designs with 128*128 pillars). The Far field modulous is calculated using FDTD, pillar-wise library (Model 0), and ResNeXt (Model 1). Arrows indicate non-negligeable zeroth orders.

One of the fascinating characteristics of these periodic convolutional neural networks is that they are not limited by the size of the training databases' inputs and outputs. They can be trained using matrices of a certain size and subsequently make predictions on larger matrices. As mentioned, the networks are trained using the previously mentioned 20x20 matrices, but they are then capable of predicting the near field for input matrices that are e.g. 128x128 in size as testified in Figure 8 and Figure 9.

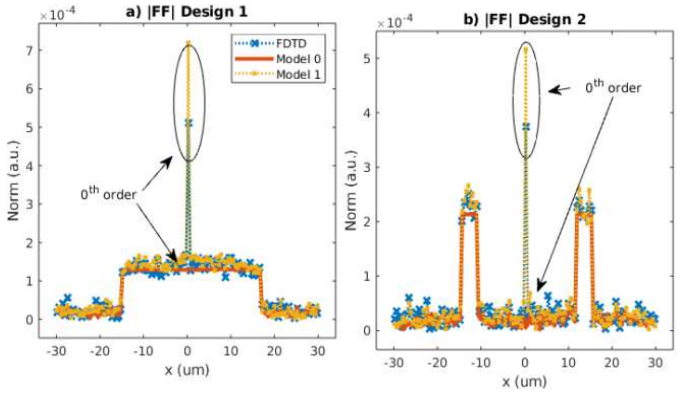

Figure 9: 2D-cuts along the x-direction of Figure 8. Arrows point out zeroth orders. Design 1 and 2 refer to the left and right colomns in Figure 8. Other legends read the same way as in Figure 8.

Two designs producing far fields of arbitrary shapes have been simulated respectively with a) and d) FDTD, b) and e) the library model, and c) and f) the present ResNeXt model. If the general shape of the far field is identical for all models, the predictions of the zeroth orders are nevertheless different depending on the model. In particular, and as can be seen on the transverse cuts of the far field (Figure 9), FDTD and ResNeXt model are aligned concerning the existence of a non-zero zeroth order while the library predicts its complete absence. It is worth mentioning that the simulation time of a CNN is significantly smaller than for FDTD: typically, a 128x128 design takes only a few seconds on a single-core machine, while it requires about 10 hours on a recent 15 cores CPU system.

V. Conclusions

The present results demonstrate the importance of precise modeling of the effect of the interaction between the pillars and allows during the design verification phases to eliminate diffusers designs that present an excessively high zero order. The use of CNN allows predicting the optical behavior of meta-diffusers or meta-lenses with sufficient precision while maintaining a satisfactory CPU execution time. These results is nevertheless more general and the same methodology can be applied to different structures such as polarized meta-structures featuring asymmetric pillars or resonating filters.

References

[1] S. So, J. Mun, J. Park, and J. Rho, "Revisiting the Design Strategies for Metasurfaces: Fundamental Physics, Optimization, and Beyond", Adv. Mater. 35, 2206399, 2023.

[2] C. Gigli, Q. Li, P. Chavel, G. Leo, M. L. Brongersma, and P. Lalanne, "Fundamental limitations of huygens' metasurfaces for optical beam shaping," Laser & Photonics Reviews, vol. 15, no. 8, p. 2000448, 2021.

[3] J. Hu, S. Bandyopadhyay, Y. Liu, and L. Shao, " A Review on Metasurface: From Principle to Smart Metadevices", doi: 10.3389/fphy.2020.586087, 2021.

[4] Lumerical Inc. , FDTD.

[5] H. Wang, W. Yue, Q. Song, J. Liu, and G. Situ, "A hybrid Gerchberg–Saxton-like algorithm for DOE and CGH calculation", Optics and Lasers in Engineering, Vol. 89, pp 109-115, 2017.

[6] S. An, B. Zheng, M. Y. Shalaginov, H. Tang, H. Li, L. Zhou, Y. Dong, M. Haerinia, A. M. Agarwal, C. Rivero-Baleine, et al., "Deep convolutional neural networks to predict mutual coupling effects in metasurfaces," Advanced Optical Materials, vol. 10, no. 3, p. 2102113, 2022.

[7] K. He, X. Zhang, S. Ren, and J. Sun, "Deep residual learning for image recognition", IEEE Conference on Computer Vision and Pattern Recognition (CVPR), 2016.